



HAL
open science

First Application of Ion Cyclotron Resonant Frequency Waves on WEST Plasma Scenarios

L. Colas, G. Urbanczyk, M. Goniche, E. Lerche, J. Hillairet, W. Helou, G. Lombard, P. Mollard, V. Bobkov, O Meyer, et al.

► **To cite this version:**

L. Colas, G. Urbanczyk, M. Goniche, E. Lerche, J. Hillairet, et al.. First Application of Ion Cyclotron Resonant Frequency Waves on WEST Plasma Scenarios. 23rd Topical Conference on Radiofrequency Power in Plasmas (RFPPC), May 2019, HEFEI, China. cea-02477474

HAL Id: cea-02477474

<https://cea.hal.science/cea-02477474>

Submitted on 13 Feb 2020

HAL is a multi-disciplinary open access archive for the deposit and dissemination of scientific research documents, whether they are published or not. The documents may come from teaching and research institutions in France or abroad, or from public or private research centers.

L'archive ouverte pluridisciplinaire **HAL**, est destinée au dépôt et à la diffusion de documents scientifiques de niveau recherche, publiés ou non, émanant des établissements d'enseignement et de recherche français ou étrangers, des laboratoires publics ou privés.

First Application of Ion Cyclotron Resonant Frequency Waves on WEST Plasma Scenarios

L. Colas^{1,a)}, G. Urbanczyk¹, M. Goniche¹, E.A. Lerche^{2,3}, J. Hillairet¹, W. Helou¹, G. Lombard¹, P. Mollard¹, V. Bobkov⁴, O. Meyer¹, J. Gunn¹, C. Desgranges¹, V. Basiuk¹, B. Pégourié¹, R. Dumont¹, J.F. Artaud¹, C. Bourdelle¹, N. Fedorczak¹, F. Durodié², J.-M. Bernard¹ and the WEST Team⁵

¹CEA, IRFM, F-13108 Saint Paul-Lez-Durance, France..

²LPP-ERM/KMS, TEC partner, Brussels, Belgium

³CCFE, Culham Science Centre, Abingdon, Oxfordshire OX14 3DB, UK

⁴Max-Planck-Institut für Plasmaphysik, Boltzmannstr. 2, 85748 Garching, Germany

⁵<http://west.cea.fr/WESTteam>

^{a)} Corresponding author: laurent.colas@cea.fr

Abstract. In 2018, Ion Cyclotron Resonant Frequency (ICRF) waves were for the first time applied to the WEST plasma scenarios. In ICRF-only plasmas at medium density, or on top of a low level of Lower Hybrid (LH) power, the coupled ICRF power increases the plasma energy content. However in discharges with large LH power at high core density, nearly all the applied ICRF power gets radiated, mainly in the plasma bulk. Both the energy content and conducted power decrease. Two peculiarities of WEST, that may combine, are presently invoked to explain this phenomenology: 1) Fast ion ripple losses, evidenced between TF coils on the baffle, likely degrade the ICRF heating efficiency. 2) RF-enhanced W sources, evidenced on several Plasma-Facing Components (PFCs), likely over-contaminate the high-power plasmas.

OVERVIEW OF THE FIRST ICRF EXPERIMENTS ON WEST

WEST [1] ($R=2.5\text{m}$, $a\sim 0.5\text{m}$) is a full-tungsten (W) diverted tokamak relying on Ion Cyclotron Resonant Frequency (ICRF) and Lower Hybrid (LH) waves for heating and current drive [2]. In view of accessing the H-mode, plasma scenarios were developed at toroidal fields $B_t=3.2\text{T}$ and 3.7T , plasma currents $I_p=300$ to 700kA , in upper and lower-single-null (USN, LSN) configurations. In 2018 ICRF waves were first applied to these scenarios, using the D[H] minority scheme at frequencies $f_0=48$, 55.5 and 57MHz . Up to 1.4MW ICRF power was coupled from two load-resilient 2×2 phased strap arrays [3]. ICRF waves were combined with up to 4.3MW LH power.

Figures 1 illustrate two types of WEST L-mode LSN discharges at $B_t=3.7\text{T}$, $I_p=500\text{kA}$, $f_0=55.5\text{MHz}$. In ICRF-only plasmas at medium density (#53778, figure 1.a), or on top of a low level of LH power, ICRF application increased the plasma energy content W_{dia} deduced from diamagnetic coil measurements. More neutrons were produced, suggesting some heating of the deuterium ions. Yet the ion temperature T_i was not measured directly. 60% to 80% of the injected ICRF power P_{IC} was evacuated as extra plasma radiation ΔP_{rad} , a similar fraction as for the ohmic power. Infrared thermography showed extra heat loads (yet not quantified) on the divertor during ICRH. This indicates an increased power P_{cond} conducted through the separatrix, despite the large radiated power fraction $\Delta P_{rad}/P_{IC}$. The ICRF heating efficiency is therefore inferred larger than 60%, although it was not evaluated directly.

In presence of a larger background LH power (P_{LH}) at higher core density (#53923, figure 1.b), the core electron temperature T_{e0} decreased faster during ICRH than just before ICRH. The core density n_e increased faster over the whole profile. The energy content slightly decreased, mainly on the electron channel. Increased neutron production

still suggests ion heating. Nearly all the applied P_{IC} was radiated, mainly in the bulk plasma, *versus* only $\sim 50\%$ of the applied P_{LH} . Yet there is no sign of impurity accumulation over several seconds of ICRF pulses. The divertor tiles cooled down both on the inner and outer strike points, indicating a reduced P_{cond} during ICRH.

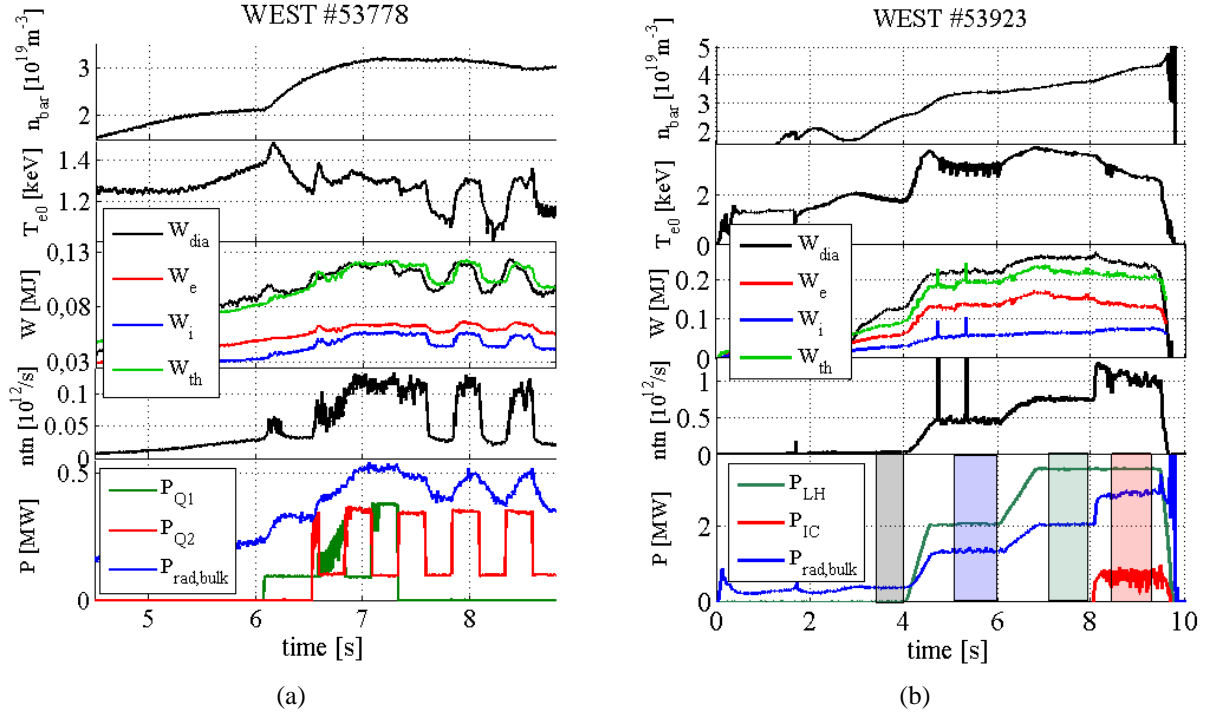


FIGURE 1. Time traces of typical ICRF-only (a) and high-power high-density (b) discharges on WEST. On the left panel the additional power was toggled between the 2 available ICRF antennas in ports Q1 and Q2. Only Q2 was active on the right panel. W_e is inferred from measured n_e and T_e profiles using interferometry and ECE radiometry. W_i is estimated from the neutron rate, assuming homothetic T_e and T_i profiles. Colored rectangles on [figure 1b](#): time windows for averaging WI line profiles in [figure 3](#).

The parametric domains for the two types of plasma discharges are hard to determine precisely. In the pulses at 3.7T/55.5MHz/500kA (the most populated database), core electron cooling appeared above ~ 1.5 - 2.5 MW of background P_{LH} . Scenario constraints generally correlate higher P_{LH} with higher core density. Only two ICRF pulses were produced at 3.7T/57MHz, in USN configuration with $P_{LH}=2.8$ MW. ICRF was applied for 4s at the middle of a 30s flat top at $I_p=300$ kA. T_{e0} decreased but the plasma recovered after ICRF switch-off. Nearly all the discharges at 3.2T/48MHz exhibited core electron heating. Most of these pulses were at $P_{LH}<1.5$ MW, but one cannot exclude an effect of the ICRF frequency. Over 5 pulses at 48MHz and $P_{LH}=0$, the minority concentration n_H/n_D was scanned by puffing H_2 *via* a dedicated valve [4]. n_H/n_D , as estimated in the SOL from the ratio of H_α over D_α spectroscopic line intensities, varied between 3% and 11%. All over this scan the discharges exhibited core electron heating.

Below we examine two peculiarities of WEST, whose combination could explain the observed phenomenology.

INDICATIONS OF MINORITY ION RIPPLE LOSSES

With only 18 toroidal field (TF) coils, the magnetic field on WEST features a ripple of $\delta B/B_r \sim 2.3\%$ at the outboard mid-plane. Ripple creates local magnetic wells that can trap the ICRF-accelerated H^+ minority ions and de-confine them before they thermalize onto bulk plasma species [5]. This degrades the ICRF heating efficiency. Although WEST plasmas were moved towards the high-field side of the vacuum chamber, WEST equilibria are more elongated and have lower I_p than those of Tore Supra. This reduces the extent of the good confinement zone for H^+ ions, such that it does not always intersect the radius R_{IH} of the H^+ cyclotron layer.

In the absence of fast ion diagnostic, ripple power losses were visualized by a wide-angle infrared (IR) camera as toroidally-modulated heat loads on the baffle (see [figure 2](#)), where trapped ions are expected to impinge. The $n=18$ modulation appeared only during ICRH and peaked between TF coils, as expected from ripple losses. Quantifying the

loss from IR thermography is delicate: the region of interest is spatially under-resolved, the IR emissivity of the W-coated baffle is ill-defined. Calorimetry could neither be used: the baffle was not actively cooled.

Bolometry line of sight (LOS) #1, aiming at the baffle between TF coils while avoiding the main plasma (see figure 2), also recorded extra radiation during ICRH. The vertically symmetric LOS #16, also avoiding the main plasma but aiming at the top of the machine, did not record any extra signal during ICRH. This up/down asymmetry was preserved when switching from LSN to USN configurations, as expected from ripple losses. The intensity of the radiation increment on LOS #1 during ICRH varied consistently with an empirical scaling law for the ion ripple power losses observed on Tore Supra [5].

$$P_{ripple} \propto P_{IC}^{1.3} \bar{n}^{-0.87} R_{1H}^{9.1} I_p^{0.2} \quad (1)$$

The correlation is illustrated on figure 2 for a subset of the WEST database at $I_p=500\text{kA}$. We speculate that the extra bolometric signal is due to fast neutrals formed by the H^+ ions hitting the baffle. While this signal may provide operational guidelines to reduce the ripple losses, it tells nothing about their absolute value. Scaling (1) does *not* predict that the fraction of P_{IC} lost in the ripple should increase drastically in high-density discharges with a large background P_{LH} .

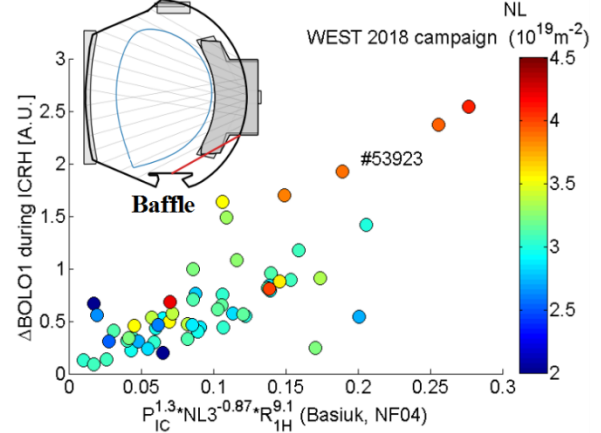


FIGURE 2. Increment of signal on bolometry LOS #1 during ICRH, vs empirical scaling (1) for WEST pulses at $I_p=500\text{kA}$. Color code: density integrated along central interferometry chord. Inset: cross section of WEST vacuum vessel with separatrix for pulse WEST #53923 during ICRH and bolometric LOS. LOSs are numbered #1—#16 from the bottom to the top of the machine. LOS#1 highlighted in red aims at the baffle.

IMPURITY CONTAMINATION AND TUNGSTEN SOURCES DURING ICRH

While they likely degrade the ICRF heating efficiency, ion ripple losses alone cannot account for the core electron cooling. Density rise and enhanced radiation also need to be invoked. During ICRH, the central bolometry LOSs exhibit a larger relative increase than the one crossing the X-point. This suggests that the extra radiation is rather central and arises from high-Z impurities. One leading candidate is tungsten (W), covering all the PFCs on WEST. Ag, present on the ICRF antenna Faraday screens, was also evidenced in the core plasma only during ICRH and could also contribute. The W concentration n_W is not measured directly. Yet an upper bound can be estimated, assuming that P_{rad} is entirely due to W and that n_W profiles are homothetic to n_e . On pulse #53923, one then needs $n_W/n_e \sim 2.8 \times 10^{-4}$ to explain P_{rad} just before ICRH. When P_{IC} is added, the impurity fraction grows to $n_W/n_e \sim 3.3 \times 10^{-4}$.

All the plasma facing components (PFCs) on WEST are tungstenized and could possibly contribute to a contamination of the plasma core. Several of them are observed with visible spectroscopy [6]. As a proxy for the gross erosion rate Γ_W on these objects, one monitors the radiance of the WI line. This does not account for a possible prompt re-deposition of the W^+ ions. Figure 3 shows the evolution over pulse #53923 of the WI line emission along the right side limiter of antenna Q2, the only active ICRF antenna on this discharge. The WI line radiance progressively grows as one goes from the ohmic to LH-only and LH+ICRH phases of the pulse. The increase during ICRH is larger than the one that would be obtained with an equivalent extra P_{LH} .

Γ_W can be expressed as the product of Γ_D (an influx of deuterium onto the PFC) by Y_{eff} (an effective sputtering yield). As a proxy for Γ_D we use the radiance of the DI_s line produced by recycled neutrals. Detailed

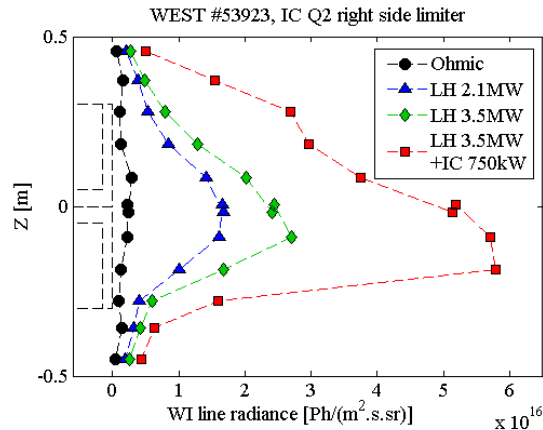


FIGURE 3. Vertical profile of the WI line ($\lambda=400.9\text{nm}$) radiance along the right side limiter of ICRF antenna Q2, averaged over 4 time windows on pulse #53923 (see figure 1). Left: sketch of WEST ICRF antenna structure.

study shows that on pulse #53923, the increase on Γ_D is

the main cause of variation for Γ_w between the ohmic and LH-only phase. This trend is partly due to the rise of the core density. Besides, figure 4 evidences a specific enhancement of the SOL density, faster than the core density, in presence of LH power. Higher edge density also improves the ICRF wave coupling on WEST [4]. Figure 5 plots the line ratio WI/DI_8 , representative of Y_{eff} . Based on this indicator, enhanced Y_{eff} is the main cause of variation for Γ_w between LH-only and LH+IC phases, when the RF voltage at the active feed ports exceeds a threshold.

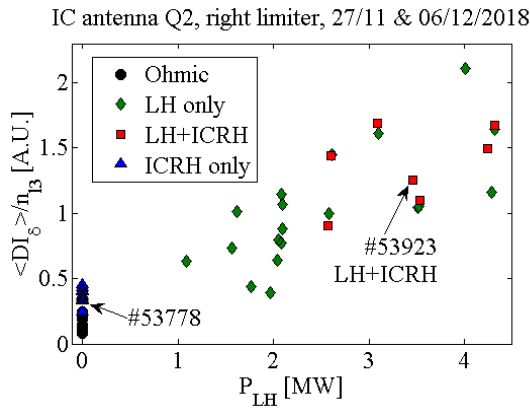


FIGURE 4. DI_8 line ($\lambda=410.1\text{nm}$) radiance averaged over time and over right side limiter of IC antenna Q2, normalized by line-integrated density, versus LH power.

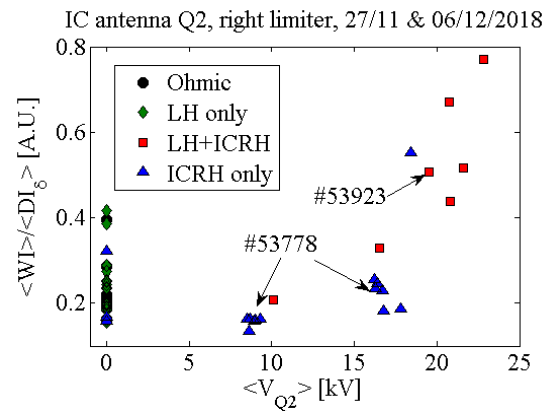


FIGURE 5. Line ratio WI/DI_8 averaged over time and over the right side limiter of ICRF antenna Q2, versus the RF voltage at the feeders of antenna Q2.

Similar behaviour as figures 3-5 is observed on the antenna protection limiter (APL, on the outboard port Q3a adjacent to antenna Q2), on the divertor but not on the left limiter of LH grill 1. For this specific limiter, located on port Q6a and not connected to the active ICRF antenna, neither Y_{eff} nor Γ_w do evolve when antenna Q2 is energized.

During the ICRF phases the WI line radiance on the IC antenna limiter is ~ 10 times higher on pulse #53923 than on #53778. This is both due to larger Γ_D (see figure 4) and larger Y_{eff} (figure 5). The impurity penetration also likely evolves between the two types of discharges. Besides, pulses with large background P_{LH} may be more contaminated with low-Z impurities than ICRF-only pulses at medium density. This may contribute to scattered data on figure 5.

DISCUSSION AND OUTLOOK

Two types of ICRF-heated discharges were evidenced on WEST. The border between them is hard to determine. ICRF affects more the energy content, the radiation and the conducted power on discharges at high density with large background P_{LH} . Unfortunately these discharges also have the highest performance before ICRH. They also ease the ICRF coupling [4]. To get a full power balance many parameters yet remain to be quantified: the ICRF heating efficiency, the conducted power, the amount of ICRF power lost in the ripple, the amount of W sputtered, its penetration. Two combined processes are presently invoked to explain the phenomenology: 1) ion ripple losses likely degrade the ICRF heating efficiency; 2) RF-enhanced W sources likely over-contaminate the high-power plasmas. To reduce ripple losses one can act on I_p , R_{1H} , n_H/n_D . The impurity mitigation strategy depends on the source location.

The contribution of each PFC to the core contamination is yet poorly known. On ASDEX upgrade [7] and EAST [4], a non-negligible contamination arose from W limiters connected magnetically to active ICRF antennas. Comparing limiters with W *versus* low-Z materials, as done in [7], would help quantifying the specific role of these components on WEST. Screening W sources while maintaining a good IC wave coupling will be investigated in the upcoming campaign. A third ICRH antenna will be installed. The goal is to reach $P_{IC}=4\text{MW}$.

REFERENCES

1. [1]: C. Bourdelle et al. *Nucl. Fus.* **55** (2015) 063017
2. [2]: A. Ekedahl et al., *AIP Conference Proceedings* **1689**, 030013 (2015); [doi 10.1063/1.4936478](https://doi.org/10.1063/1.4936478)
3. [3]: W. Helou et al., invited paper I2.9, this conference.
4. [4]: G. Urbanczyk et al., invited paper I3.5, this conference.
5. [5]: V. Basiuk et al. *Nucl. Fusion* **44** (2004) p.181
6. [6]: O. Meyer et al., *Rev. Sci. Instrum.* **89**, 10D105 (2018); <https://doi.org/10.1063/1.5035566>
7. [7]: V. Bobkov et al. *Nucl. Fusion* **53** (2013) 093018